IEEE Open Journal of the
Industrial Electronics Society

Received 24 May 2024; revised 12 June 2024; accepted 12 June 2024.
Date of current version 24 June 2024. The review of this article was arranged by Associate Editor S. Golestan.

Digital Object Identifier 10.1109/OJIES.2024.3415007

Mixed Redundancy Strategy for Modular Multilevel Converters in High-Power Applications

MIAD AHMADI (Student Member, IEEE), ADITYA SHEKHAR (Member, IEEE), AND PAVOL BAUER (Senior Member, IEEE)

Delft University of Technology, Department of Electrical Sustainable Energy, DCE&S Group, 2628, CD Delft, The Netherlands

CORRESPONDING AUTHOR: MIAD AHMADI (e-mail: m.ahmadi-3@tudelft.nl)

ABSTRACT Modular multilevel converters are favorable for efficiently operating high-power usages. The required number of components significantly increases when higher modularity is introduced for the given voltage level, thus reducing the system's reliability. This article suggests a mixed redundancy strategy (MRS) that combines the operational concepts using active and spare redundant submodules. It is shown that more than 50% higher B10 lifetime (the point in time when the system has a 90% probability of survival) is achievable as compared to reliability improvement using fixed-level active redundancy strategy, load-sharing active redundancy strategy, and standby redundancy strategy with the same number of redundant submodules. The tradeoff between operational efficiency and investment cost is explored to define the boundary for selecting the MRS over other redundancy strategies with varying dc-link voltages and average converter loading, considering a ten-year payback period and equivalent B10 lifetime. The change in viability boundary for the MRS is established with increasing B10 lifetime and its sensitivity to power electronic component costs and assumed failure rate. The effect of power capacity with a higher switch current rating is evaluated. Also, the Monte Carlo simulation methodology is proposed to evaluate the practicality and effectiveness of the proposed MRS scheme. Finally, the insights of this study are applied to existing literature.

INDEX TERMS Cost assessment, mixed redundancy, modular multilevel converter (MMC), Monte Carlo simulation (MCS), redundancy methodologies, reliability analysis.

NOMENCLATURE

Variables

ΔCI	Variation in capital investment between redundancy strategies.
ΔE_i	Difference in cost savings between redundancy strategies.
$\eta(t_i)$	Efficiency.
$\lambda_{\text{base-Cap}}$	Capacitor base failure rate.
$\lambda_{\text{base-IGBT}}$	IGBT base failure rate.
λ_x	Failure rate of different components.
B_{10}	Point in time when the system has a 90% probability of survival.
$CI_{\text{N-WoR}}$	Normalized CI without redundancy.
$CI_{\text{N-WR-x}}$	Normalized CI with redundancy for various switch ratings.
$CI_{\text{N-WR}}$	Normalized CI with redundancy.
CI_{WoR}	Total CI without redundancy.
E_{l}	Yearly energy losses.
k	Minimum number of SMs.
k_x	Minimum number of SMs for different switch ratings.
k_{max}	Capacitors voltage ripple.
MTTF	Mean time to failure.
n_{A}	Number of active redundant SMs within each arm (for MRS).
N_{red}	Number of redundant SM in each arm for SRS, FL-ARS, and LS-ARS.
n_{S}	Number of spare redundant SMs (for MRS).
$N_{\text{T-Red}}$	Total of redundant SM for different redundancy strategies.

P_{ave}	Annual average loading.
P_t	Electricity price.
$R(t)$	Reliability function.
$R_{arm\text{-}x}(t)$	Arm reliability function with various redundancies.
S_f	Safety factor of IGBT.
S_{MMC}	Rated power.
$T_{O\&M}$	Maintenance period.
V_{dc}	DC-link voltage.
V_{IGBT}	IGBT rated voltage.
S_i	Disparity in energy savings between redundancy strategies.

Acronyms

CI	Capital investment.
FIT	Failure in time.
FL-ARS	Fixed-level active redundancy strategy.
FR	Failure rate.
HV	High voltage.
IGBT	Insulated gate bipolar transistor.
LS-ARS	Load sharing active redundancy strategy.
MCS	Monte Carlo simulation.
MMC	Modular multilevel converter.
MRS	Mixed redundancy strategy.
MV	Medium voltage.
O&M	Operation and maintenance.
SM	Submodule.
SRS	Standby redundancy strategy.

I. INTRODUCTION

MMCs are used in MV, HV, and high-power applications to achieve an efficient and scalable solution with improved power quality [1], [2].

Extensive research relevant to MMC's control, modeling, configuration, and protection strategies has been carried out [3], [4]. In grid-connected power electronic converters, reliability evaluation is mostly carried out by focusing on three distinctive levels, namely, component [5], [6], converter, and power system, to enhance reliability. At the component level, the mission profile and physics of the components (power switches and capacitors) are targeted to improve reliability. At the converter level (this study focus), various methodologies, such as redundancy, modularity, and reconfigurability, are used to enhance reliability [7]. At the power system level [8], [9], [10], reliability improvement is achieved by applying different methods, such as protection and $n-1$ contingency design.

Safe and seamless operation of the MMC system is paramount and represents the primary focus of reliability studies. To address this concern, redundancy concepts, as outlined in various studies [11], [12], [13], [14], [15], [16], have been established as effective methods for ensuring normal postoperation in the MMC when SMs encounter failures. Several strategies exist for managing redundant SMs.

1) *FL-ARS:* It is also known as hot-reserved redundancy; only k SMs are active, while redundant SMs remain powered. The triggering signal randomly activates k SMs, ensuring that all SMs take turns operating.
2) *SRS:* It is known as cold-reserved redundancy; k SMs are always active, while redundant SMs remain idle. An active SM is bypassed upon failure, and the redundant SM will start operating.
3) *LS-ARS:* In this redundancy strategy, the redundant SMs are operational, distributing the load among $k + N_{red}$ SMs, resulting in a lower operating voltage for each SM than SRS and FL-ARS.

It is crucial to acknowledge that implementing redundancy involves additional upfront investment and potential operational losses, comprehensively addressed in [17], [18], [19], and [20]. For example, in [12], a reliability model is presented for MMCs, comparing two SM types, concluding that the individual device SM is most efficient for converter reliability and power loss. Xu et al. [13] introduce a reliability analysis model for hybrid MMCs and propose new principles to optimize the design of redundant SMs, ultimately enhancing overall system reliability. Xie et al. [15] give detailed reliability models for hybrid MMCs in different applications, including active and passive redundancy schemes. In [17], a systematic criterion for selecting multilevel converters is outlined for MV applications, considering reliability, redundancy, efficiency, and cost factors.

Modularity, as highlighted in [21], [22], and [23], represents another critical concept that significantly influences the reliability, efficiency, and overall cost considerations of the MMC. Ahmadi et al. [23] present a methodology for selecting the optimal switch voltage in MMCs based on cost and reliability tradeoffs, showing that it depends on factors such as dc-link voltage, average loading, and component reliability estimation methods. Huber and Kolar [21] discuss selecting the number of cells in the converter for MV applications, considering tradeoffs in efficiency, power density, and reliability. Redundancy options are also explored, providing a comprehensive perspective for designing high-power MV converter systems. In [22], a reliability-focused design methodology is proposed using a case study of a 17-MVA/13.8-kV MMC. It demonstrates that 3.3-kV devices offer the best tradeoff.

The maintenance concept [19], [24], [25], [26] for MMC is crucial to avoid unscheduled outages. It encompasses preventive, periodic, and protective maintenance. Planned maintenance involves replacing faulty SMs within the MMC structure. However, this maintenance necessitates a system shutdown, incurring substantial costs and requiring thorough planning. In [24], a reliability-centered maintenance approach is elaborated with dual redundancy, optimizing maintenance intervals based on dynamic operation states. This model aids in choosing redundancy strategies and maintenance decisions. In [19], a reliability model incorporates preventive maintenance; the model evaluates reliability indices, maintenance intervals, and cost considerations, indicating the choice between SRS and LS-ARS. Feng et al. [25] introduce a dynamic preventive maintenance strategy in wind power systems, optimizing redundancy and maintenance intervals to reduce costs

TABLE 1. REVIEW OF THE EXISTING RELIABILITY-RELATED DESIGN OF THE MMC

Reference	Red†	Mod‡	Maintenance	Cost	Gen§
[12]–[16]	✓				
[17]	✓			✓	✓
[18]–[20]	✓			✓	
[21]	✓	✓			✓
[22]		✓		✓	
[23]	✓	✓		✓	✓
[24]–[26]	✓		✓	✓	
[27]	✓		✓		
This paper	✓	✓	✓	✓	✓

† Redundancy ‡ Modularity
§ Generalization (various MMC characteristics)

TABLE 2. MMC Characteristics and FRs

Symbols	Value
k_x	—†
V_{dc}	10 - 400 kV
S_{MMC}	5.9 - 235.3 MVA
V_{IGBT}	x ∈{1.2, 1.7, 3.3, 4.5, 6.5} kV‡
k_{max}	10%
S_f	0.65
$\lambda_{base\text{-}IGBT}$	100 FIT [20]
$\lambda_{base\text{-}Cap}$	100 FIT [20]

† Changes based on the selected IGBT rated voltage
‡ Switch models are given in Appendix

while maintaining reliability. Table 1 presents an overview of previous research endeavors documented in the literature. In this study, a comprehensive examination of MMC design is undertaken by applying a new redundancy strategy, encompassing facets such as redundancy, modularity, maintenance, cost considerations, and generalization, including considering different dc-link voltage and loading scenarios.

This article introduces the MRS, and Section II provides a comprehensive explanation of its operational principles. In the MRS operational mode, two important parameters come into play: n_A and n_S available for the MMC. During maintenance procedures, these spare SMs can substitute faulty SMs across all arms. The MRS suits various MMC applications, including those with different maintenance planning, dc-link voltage, and annual average loading. MRS determines the optimal number of n_A in each arm and accurately estimates n_S, the number of spare SMs slated for replacement during maintenance. This allows for consideration during the initial design phases, enabling a more accurate estimation of the capital cost, encompassing cost, redundancy expenses, and the number of spare SMs designated for replacement. Therefore, based on the characteristics of the system, such as defined dc-link voltage, loading, and maintenance schedule, MRS ensures an optimized selection. It allows for the minimization of n_A based on the maintenance frequency, resulting in reduced capital costs, operational losses, and control simplicity (achieved by utilizing fewer SMs).

This work presents the following key contributions.

1) This article develops a reliability assessment method for the proposed scheme and validates it using the MCS method (see Section II).
2) It establishes the economic viability boundary for the proposed scheme with varying V_{dc} and average annual loading by investigating the tradeoff between investment cost, operational losses, and reliability (see Section III).
3) It defines generalized viability boundary for MRS using sensitivity to changes in B_{10} lifetime requirement, component FR, cost, and power capacity (see Section IV).
4) It recommends the optimal arm-level redundancy, maintenance frequency, and replacement criteria for the proposed scheme considering different scenarios (see Section V).

The main conclusions of the study are presented in Section VI.

II. METHODOLOGY

A. SYSTEM DESCRIPTION AND ASSUMPTIONS

In Table 2, the characteristic of the considered system is shown.

k_x that are required for each arm is estimated as follows:

$$k_x = \text{Ceil}\left[\frac{k_{max} \times V_{dc}}{S_f \times V_{IGBT}}\right]. \tag{1}$$

The IGBTs and capacitors are the main high-power SM components that play a key role in the converter's operation and are relatively more prone to failure while contributing significantly to the cost and size of the system. For the cost evaluation, the system considered in [27] is used, in which the IGBT module from Infineon Technologies, FF450R33T3E3BPSA1-ND, with a withstand voltage of 3.3 kV is used. For the capacitor bank, a series connection of four capacitors of KEMET, ALS71C133QT500-ND, with 500 V and 13 mF is considered to provide an SM capacitance of approximately 3.3 mF in accordance to the MMC designed in [28] based on the method presented in [29].

During the operational lifespan, the FR of IGBT and capacitors depends on the temperature and voltage across them. Hence, these limitations need to be considered in the FR formula of the IGBT and capacitors [30] that are detailed in [23] and are not repeated here. The FR of other auxiliary devices, including fuses, low voltage power supply, gate drive, cooling, and control system, also influences the converter life. These impacts are explored in Section IV employing the sensitivity of derived results to the higher FR.

B. WORKING PRINCIPLE OF MRS

The arm's reliability block diagram in the MRS working mode is shown in Fig. 1. In this scheme, spare SMs (n_S) are not physically connected to the arms, and active redundant SMs in arms are operating identically to the LS-ARS, eliminating any added complexity to the system. However, this scheme aims to minimize the number of n_A in each arm. During maintenance, the spare SMs replace faulty SMs, as illustrated in Fig. 1. The maintenance frequency in the MRS is determined by the count of active redundant SMs in each arm (n_A). For instance, if $n_A = 1$, maintenance is scheduled upon the failure of a single SM in any arm. This strategy ensures continuous operation since there are still k SMs in the arm, allowing for timely maintenance planning.

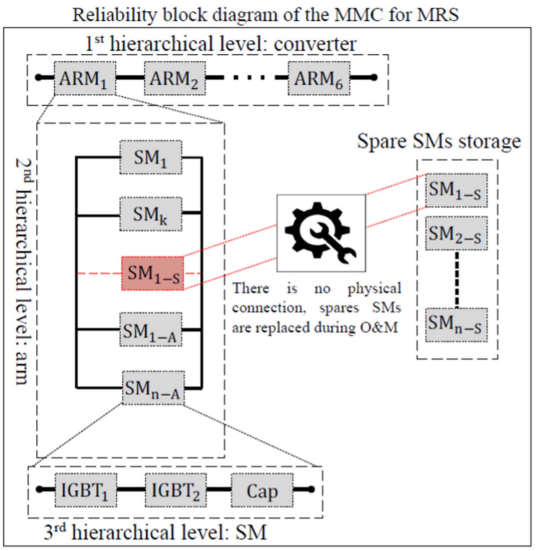

FIGURE. 1. Reliability block diagram of MMC's arm with MRS working mode.

In MMC applications, if less frequent maintenance is expected, the MRS scheme estimates that more active redundant SMs (n_A) in each arm are required. However, n_A remains significantly lower than conventional redundancy strategies. For instance, with $n_A = 3$, maintenance occurs after the third failure in any arm, providing a planned operational period with k SMs until maintenance. Simultaneously, other faulty SMs in different arms are also replaced by spare SMs n_S during maintenance.

So, there can be different combinations of active per arm (n_A) with spare (n_S) redundant SMs at the converter level in the MRS, which will be determined based on the planned maintenance frequency and number of the levels explored in Section IV. The procedure for determining $n_A = 1$ and $n_S = 4$ is shown in Fig. 2, where only one arm is shown, but spare SMs can be used in other five arms, which are not shown. The arm initially will work with ($k + n_A$) level (a). When there is one SM failure (b), the maintenance will be performed shortly (c), and this chain of process (d)–(f) continues until there is no spare SM in the storage (g). Hence, the arm will always be working with ($k + n_A$) level until there is no spare SM in the storage (a)–(g). After that, if another SM fails (h) in an arm, the arm's operation level will be k (i). Ultimately, with one more SM failure in the k-level operating arm (j), the converter will need to be shut down, and the converter will be out of operation (l).

C. RELIABILITY ASSESSMENT OF MRS

The reliability is estimated based on an instantaneous changeover similar to the methodology followed in [16] and [20]. The concept of standby systems in [17] and [31] can be applied to model the system behavior. According to the reliability block diagram model of the MRS shown in Fig. 1 and the assumptions regarding the proposed scheme's working principle, the reliability can be calculated by applying the joint failure density approach. Therefore, considering all the events that lead to system success are mutually exclusive, the reliability function under the MRS working mode can be calculated by adding the mutually exclusive events. Considering the MMC in the MRS mode, two events that led to the system's success shown in Fig. 2 are as follows.

1) *Event 1:* The MMC is operational for the time interval of 0 to t with $k + n_A$ level, and by each SM failure, one spare SM is substituted in a short time (if $n_A = 1$).
2) *Event 2:* At time t_1, the last spare SM has been substituted, and there is no spare SM left, so there are only $k + n_A$ SMs left in each arm and the MMC operates with n_A active redundant SM for time interval t_1 to t.

Fig. 3(a) and 3(b) shows the graphically represented reliability functions $R_1(t)$ and $R_2(t)$ for events 1 and 2, respectively.

$R_1(t)$ is mathematically given by (2) using the Poisson distribution with n_s spare redundant SMs

$$R_1(t) = P[N(t) \le n_s] = \sum_{i=0}^{n_s} \frac{(\lambda_{sc} t)^i}{i!} e^{-\lambda_{sc} t} \tag{2}$$

$$\lambda_{sc} = (\lambda_{IGBT\_1} + \lambda_{IGBT\_2} + \lambda_{cap}) \times 6 \times (k + n_A). \tag{3}$$

Note that (2) is also used to estimate the arm's reliability with SRS by substituting (3) with (4) as follows:

$$\lambda_{sc} = (\lambda_{IGBT\_1} + \lambda_{IGBT\_2} + \lambda_{cap}) \times k. \tag{4}$$

The derivative of $R_1(t)$ at t_1 gives the probability of n_s failures, with which the reliability function $R'(t - t1)$ with active-only modules without any remaining spares SMs is weighted to estimate $R_2(t)$ as follows:

$$R_2(t) = \int_{t_1=0}^{t} -\frac{d}{dt_1} R_1(t_1) \times R'(t - t_1) dt_1. \tag{5}$$

Note that with $t1 = 0$, $R'(t)$ can be estimated using the Markov Chain method from [16] to calculate the reliability with the LS-ARS. Since the two events $R_1(t)$ and $R_2(t)$ are mutually exclusive, the MMC reliability with the MRS (R_{MRS}) can be calculated as

$$R_{MRS}(t) = R_1(t) + R_2(t). \tag{6}$$

D. VALIDATION OF MRS USING MCS

To assess the reliability of employing the MRS, an analytical method is developed in Section II-C. Due to the absence of comparable methods in the previous literature, the MCS is employed to validate the obtained analytical results. The outcomes are visually presented in Fig. 4 for 1000 and 10 000 trials, respectively. It demonstrates the efficacy of the proposed analytical equation for calculating the reliability by applying the MRS.

E. OPTIMAL COMBINATION OF ACTIVE REDUNDANT AND SPARE SMS IN THE MRS

In the MRS, different combinations can be selected between the number of active redundant and spare SMs. For example,

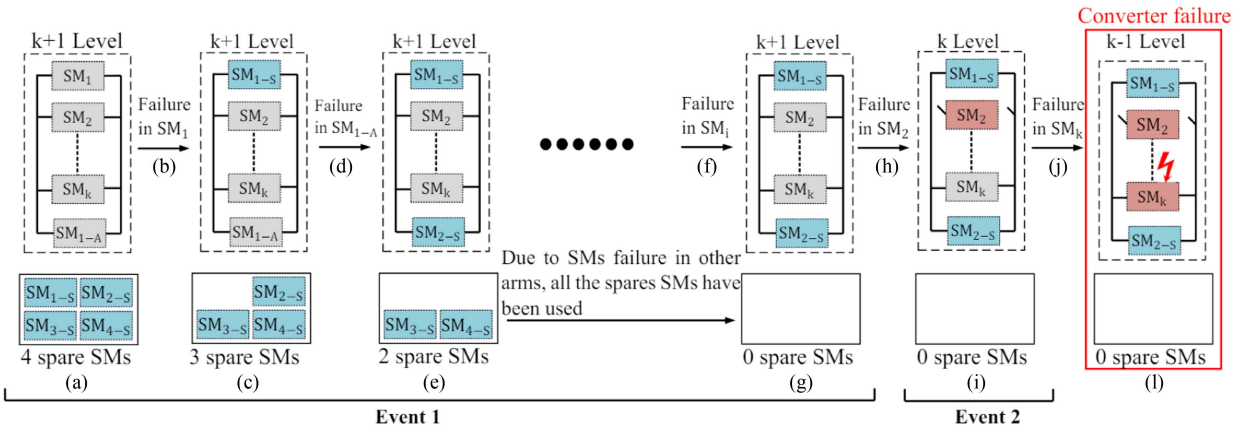

FIGURE. 2. Steps of implementing MRS in one arm of the MMC. (a) healthy condition (No. operational SMs: k + 1, No. available spare SMs: 4), (b) transition of replacing faulty SM_1 with spare $SM_{1\text{-}S}$ during maintenance, (c) healthy condition (No. operational SMs: k + 1, No. available spare SMs: 3), (d) transition of replacing faulty $SM_{1\text{-}A}$ with spare $SM_{2\text{-}S}$ during maintenance, (e) healthy condition (No. operational SMs: k + 1, No. available spare SMs: 2), (f) the same sequence of events in other arms that uses the remaining spare SMs, (g) healthy condition (No. operational SMs: k + 1, No. available spare SMs: 0), (h) transition of using redundant SM, (i) healthy condition (No. operational SMs: k, No. available spare SMs: 0), transition of another failure in SM_k that leads to (l) converter failure.

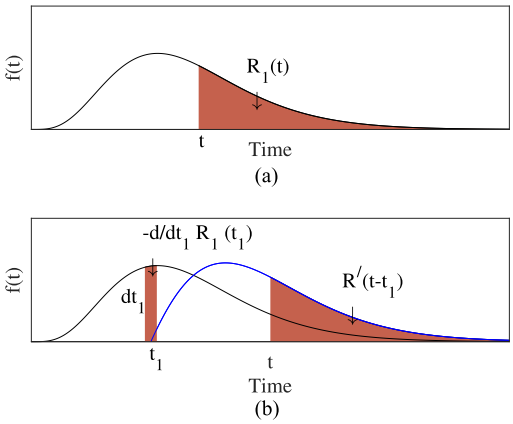

FIGURE. 3. Graphical representation for reliability functions. (a) $R_1(t)$ corresponding to event 1. (b) $R_2(t)$ corresponding to event 2.

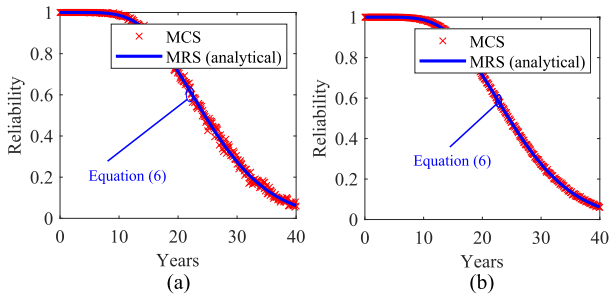

FIGURE. 4. Validation of the proposed scheme using MCS with (a) 1000 trials and (b) 10 000 trials.

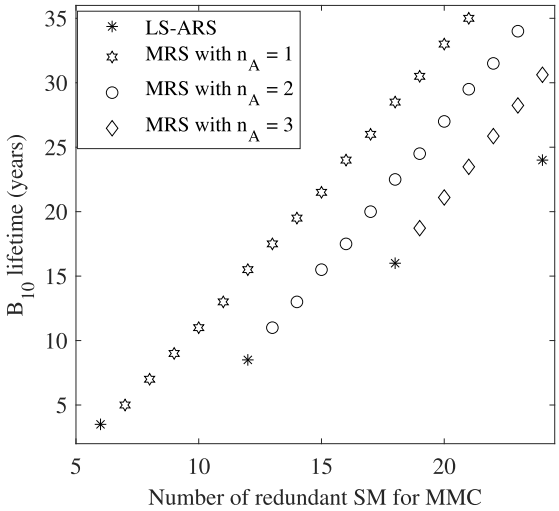

FIGURE. 5. B_{10} lifetime of the MMC with various combinations of active and spare redundant SMs in the MRS.

in the MMC with 10 MVA, and 17 kV V_{dc}, results for three combinations are presented in Fig. 5. It can be seen that having one active redundant SM in each arm and storing the rest as spare SMs shows the best reliability outputs. For instance, if the required B_{10} lifetime is 20 years, this requirement can be met with 15, 18, and 20 SMs with n_A equal to 1, 2, and 3. This is because, with only one active redundant SM, more spare SMs can be shared among the arms.

For the MMCs with very high levels of modularity, more than one redundant SM can be active in each arm. In such cases, the optimal combination can be found based on various indicators such as preventive maintenance plans and requirements. In the subsequent section, the reliability of the considered system is compared between conventional redundancies and the proposed scheme.

III. CASE STUDIES FOR COST AND OPERATIONAL EFFICIENCY TRADEOFFS

In this study, the aim is to validate the applicability of the MRS in both MV and HV applications. Two systems documented in existing literature [27], [32] are considered to achieve this. Details for each system are provided in Table 3.

TABLE 3. CHARACTERISTICS OF TWO CASE STUDIES

Item	MV	HV
V_{dc} (kV)	17	320
V_{IGBT} (kV)	3.3	3.3
k	9	200
Redundant per arm	2	16
Switching frequency (Hz)	313	150

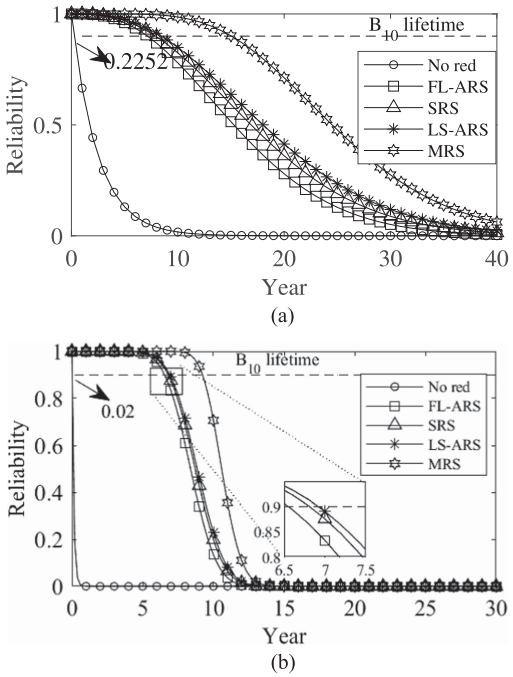

FIGURE. 6. Reliability outputs for two considered MMCs with dc-link voltage of (a) MV and (b) HV.

A. RELIABILITY OUTPUTS

Taking the systems given in Table 3, Fig. 6 shows the reliability results with different redundancy strategies. The MV system implements redundancy with two redundant SMs per arm, totaling 12 SMs. In the FL-ARS, LS-ARS, and SRS, both redundant SMs are present in each arm. Conversely, in the MRS, parameters are set as $n_A = 1$ and $n_S = 6$. In the HV scenario, conventional redundancy strategies entail 16 redundant SMs in each arm. However, the MRS scheme specifies $n_A = 4$ and $n_S = 12 \times 6 = 72$. Why these specifications are selected will be scrutinized in Section V.

From Fig. 6(a), it can be observed that B_{10} lifetime corresponding to 90% reliability (dashed black) increases from 0.2 years (no redundancy, circle marker) to approximately 10 years when two redundant SMs are considered per arm with FL-ARS (square), SRS (triangle), and LS-ARS (asterisk). This value almost doubles when the proposed MRS (hexagon) is employed with the same number of redundant SMs in the MV system. Fig. 6(b) shows that applying the MRS scheme with the same number of redundant SMs as conventional redundancy strategies will boost the lifetime corresponding to 90% reliability from 6.5 to 9.2 years.

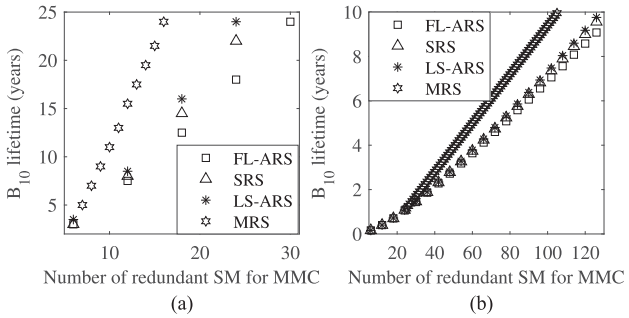

FIGURE. 7. B_{10} lifetime of the MMC with various redundancy schemes for (a) MV and (b) HV.

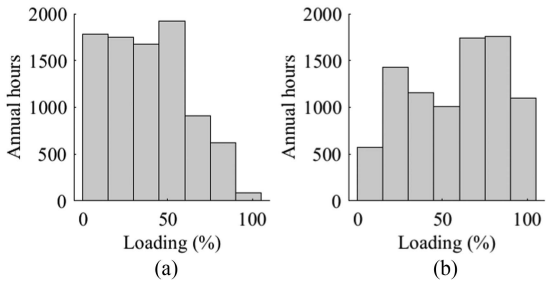

FIGURE. 8. Yearly power demand for annual average loading (P_{ave}) of (a) 38% and (b) 57% [33].

Fig. 7 shows the increase in achieved B_{10} lifetime with the increasing number of redundant SMs for different strategies in both cases of MV and HV systems. The higher impact of MRS is visible from the higher slope of the B_{10} lifetime as a function of redundancy. Since the number of redundant SMs can only be a multiple of six for conventional redundancies, the flexibility of choosing the redundancy level to meet the required reliability targets can be an advantage of the proposed scheme.

B. OPERATIONAL EFFICIENCY

In this section, the operational efficiency of different redundancies is compared using the normalized loading profile adapted based on the available hourly data of a substation in The Netherlands [33] shown in Fig. 8. The yearly energy losses of MMC with various applied redundancies can be calculated as

$$E_{l_Y} = \int (100 - \eta(t_i)) \times S_{\text{MMC}} \tag{7}$$

Where Y specifies the redundancy type, E_{l_Y} is in watthour, and S_{MMC} is in megawatt.

Fig. 9(a) presents normalized switching and conduction losses for different redundancy strategies for the corresponding loading in the MV system. The efficiency of the MV system is presented in Fig. 9(b), where SRS has the lowest losses compared to other redundancy strategies. The same results are shown for the HV system in Fig. 9(c) and 9(d). E_l of

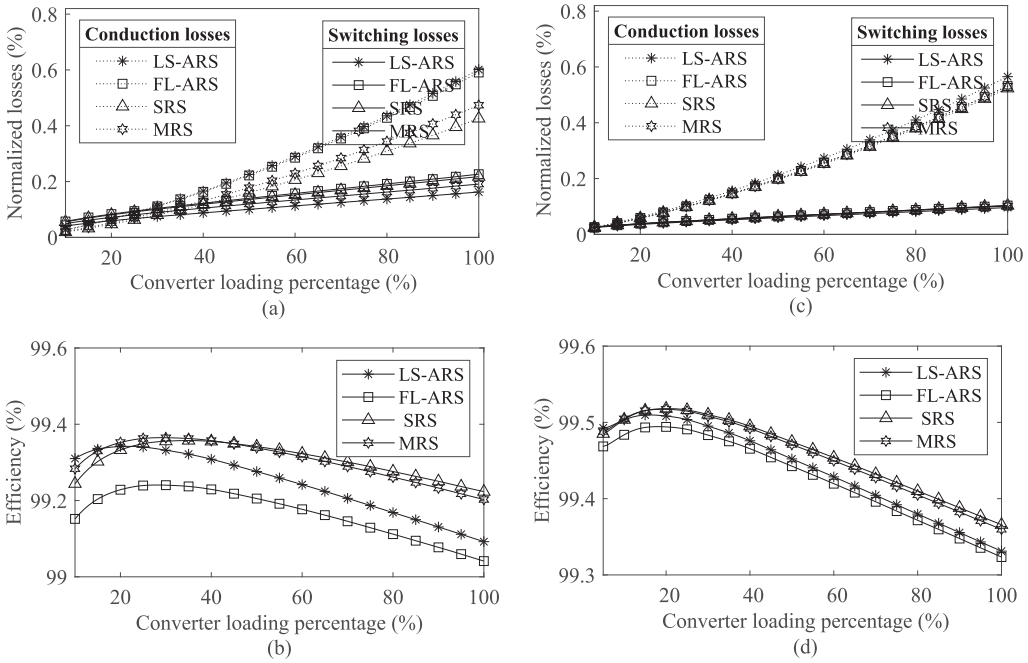

FIGURE. 9. Operational losses of the MMC for (a) switching and conduction losses in MV, (b) efficiency in MV, (c) switching and conduction losses in HV, and (d) efficiency in HV, under various redundancy modes and loading.

TABLE 4. E_l INMWH(B_{10} = 10 YEARS)

Type	Annual P_{ave}	LS-ARS	FL-ARS	SRS	MRS
MV	38 %	252.2432	265.3572	231.4225	231.9384
MV	57 %	400.6433	443.6719	355.5387	360.3674
HV	38 %	3508.55	3532.81	3377.12	3397.54
HV	57 %	4901.44	4926.25	4791.02	4803.52

TABLE 5. *CI* IN EURO OF 10-MVA 17-kVMMC WITHOUT REDUNDANCY

Components	Total cost
IGBT	85542.4
Gate Drive	9737.82
Heat Sink	9409.66
Total Capacitance	23399.28
Power Supply	5731.34
Sensors	2038
Control Board	1670
(O&M)	10%
Design cost	30%
CI_{WoR}	192539.9

various redundancy schemes concerning both case studies of annual loading (see Fig. 8) are given in Table 4 for $B_{10} = 10$ years. The information gleaned from Fig. 9 and Table 4 indicates that the MRS has lower losses in comparison to the ARS, primarily due to its utilization of a reduced number of n_A in each arm. Notably, the efficiency of the MMC tends to be higher when the SRS is employed. For applications considering the use of SRS, the efficiency aspect becomes significant. The applicability of the MRS in such scenarios is examined in Section IV.

The energy savings slightly differ when a fixed loading represents the yearly average of the hourly demand variation of the two case studies. For example, in the MV system, 5.76-MWh annual savings are estimated when the SRS is used instead of the MRS with a fixed loading of 57%, as compared to 4.83 MWh from Table 4, where hourly annual load profile is considered. The former is used in the subsequent section to simplify the computation effort required for the sensitivity analysis in defining the economic viability boundaries of the proposed scheme.

C. INITIAL COST

The CI, design, and O&M costs are relevant factors for selecting a proper redundancy scheme. Since different switches are used for various loading and V_{dc}, the cost (€/kVA) is first estimated for the base system and by using the price of the switch voltage rating of 3.3 kV. Then, it will be used to estimate the CI with various switches. The most recent price of components of the MMC with 3.3 kV rated switch to calculate the CI is as follows. The IGBT price is €1584.12 per unit, the gate drive price is €180.32 per unit, and the capacitor price is €108.33 per unit. Table 5 summarizes CI without considering redundancy. Furthermore, the design cost price is around 30% of the total cost.

The following steps can be followed to estimate the total CI, including redundancy and switch ratings

$$\mathrm{CI_{N\text{-}WoR}} = \frac{\mathrm{CI_{WoR}}}{S_{\mathrm{MMC}}(\mathrm{kVA})} \tag{8}$$

$$CI_{\mathrm{N\text{-}WR\text{-}x}} = \frac{CI_{\mathrm{N\text{-}WOR}}}{k_x \times 6} \times (k_x \times 6 + N_{\mathrm{T\text{-}red}}) \tag{9}$$

$$N_{\mathrm{T\text{-}red}} = \begin{cases} N_{\mathrm{red}} \times 6, & \text{for FL, SRS, LS} \\ 6 \times n_A + n_S, & \text{for MRS} \end{cases} \tag{10}$$

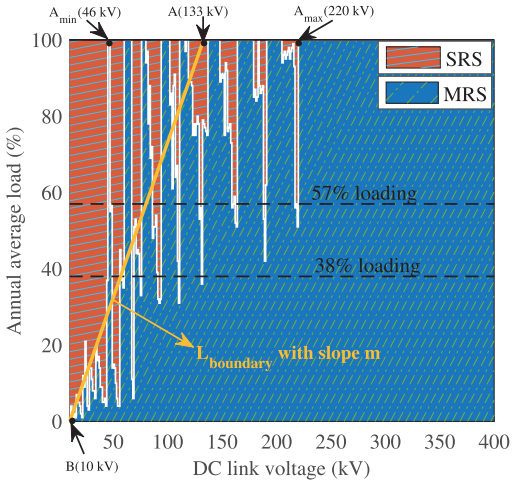

FIGURE. 10. Feasibility boundary for SRS and MRS as a function of yearly average loading and V_{dc} (payback = 10 years, B_{10} = 10 years).

where CI_{WoR} is from Table 5 in €, $CI_{\text{N-WoR}}$ is in €/kVA, and $CI_{\text{N-WR-x}}$ is in €/kVA for various switches ($x \in \{1.2, 1.7, 3.3, 4.5, 6.5\ \text{kV}\}$), and $N_{\text{T-red}}$ is defined in (10). Hence, the normalized price, including redundancy, can be obtained. The cost of MMC with MRS is lower than the other three redundancy schemes due to the MMC's lower number of redundant SMs.

D. PAYBACK

To evaluate the simple payback, the CI and the saving of various redundancies are compared to select the most economical redundancy strategy using the following equations:

$$\text{Payback} = \frac{\Delta CI}{S_{\text{i}}} \tag{11}$$

$$S_{\text{i}} = \int \Delta E_i \times P_{\text{t}} \tag{12}$$

where ΔE_i is in kilowatthour, and P_{t} is equivalent to 0.190 €/kWh.

IV. VIABILITY BOUNDARIES OF THE PROPOSED MRS

As highlighted in Section III-B, in scenarios where the application of the SRS is feasible, the efficiency advantage of SRS over the MRS is acknowledged. Consequently, the suitability of the proposed scheme is evaluated. Also, it is crucial to note that this comparison is made between the SRS and the MRS because Tables 5 and 4 and Figs. 6 and 7 suggest that the LS-ARS and the FL-ARS are less economically viable than the MRS with the considered assumptions. When the ARS is the chosen redundancy scheme, the MRS consistently emerges as the optimal choice due to its lower CI and higher efficiency. Fig. 10 shows the boundary of economic viability (L_{boundary}) between the SRS and the MRS for $B_{10} = 10$ years as a function of V_{dc} (10–400 kV) and loading (1–100%) considering a ten-year payback. Notably, within the 10–100 kV range, other multilevel converter options can rival the MMC. However, this study exclusively delves into MMC, and for a comprehensive comparison, Abeynayake et al. [17] give detailed findings. The optimal switch selected for each voltage level differs based on our previous work [23]. For example, a 1.7-kV switch is used for low loading below 50-kV dc link, while 3.3 kV is used in the 50–100 kV and 6.5 kV is used above about 200 kV. The current and voltage ratings of each IGBT and capacitor are kept fixed. The right-side region of L_{boundary} (dash-dotted line blue) indicates the operating conditions where the MRS is more economically viable. The left-side region of L_{boundary} (solid line red) corresponds to the extra investment for the SRS. It has a payback of ten years due to better efficiency than the MRS for the given dc-link voltage and average annual loading.

A linearized general equation defined based on the two points of A and B for L_{boundary} is shown in Fig. 10, given as follows:

$$\begin{cases} \text{if } \frac{\text{Loading}}{100} - m(V_{\text{dc}} - V_{\text{ref}}) \geq 0, & \text{select SRS} \\ \text{else}, & \text{select MRS}. \end{cases} \tag{13}$$

The parameters m and V_{ref} are provided in Table 6.

A. SENSITIVITY ANALYSIS

Sensitivity analysis describing the shift in this defined L_{boundary} with respect to different B_{10} lifetime requirements, FR, CI (P_{t}), and O&M is presented in Fig. 11(a)–11(d), respectively. In Fig. 11(a), it can be observed that the MRS becomes more economically viable with the increase in B_{10} lifetime requirements. For example, the SRS is preferred for both 38% and 57% loading with a 40 kV V_{dc} if the required B_{10} lifetime is five and ten years, while the MRS is viable when the required B_{10} lifetime is increased to 20 years. Fig. 11(b) suggests that there is a limited dependence of the L_{boundary} on the MMC loading when a higher FR is considered. However, the L_{boundary} shift becomes loading dependent with lower FR. Fig. 11(c) shows that the MRS will become more economically viable if the power electronic components are more expensive as compared to the reference converter costs considered in Table 5. For example, the MRS is preferred over the SRS for the two considered case studies with 40-kV dc link only when considered component costs are 20% higher. Finally, Fig. 11(d) suggests that if the O&M cost of the MRS is higher, it will become less viable. Since O&M in practical scenarios is important, this aspect is explored more in detail in Section V.

B. SENSITIVITY TO CONVERTER POWER CAPACITY

In this section, the impact of the higher power rating of the MMC is evaluated. Initially, a fixed current rating of 480 is employed, and the power of the MMC varies from 6 to 235.3 MVA by changing the dc-link voltage from 10 to 400 kV. The switch types used for this system are provided in the Appendix (see Table 9). To evaluate the impact of power rating, an evaluation is conducted with an increased current rating of the converter set to 960 A. For this case, the change in V_{dc} between 10 and 400 kV will increase the power

TABLE 6. SPECIFICATIONS OF (13)

	L_{boundary}	B_{10} (years)		FR		CI (or Pt)		O&M of MRS	
		5	20	+20%	-20%	+20% (-20%)	-20% (+20%)	+20%	-20%
m (μ)	8.13	9.3	16.7	7.8	50	10.9	12	5	14.7
V_{ref}(kV)	10	110	0	10	123	0	104	117	0

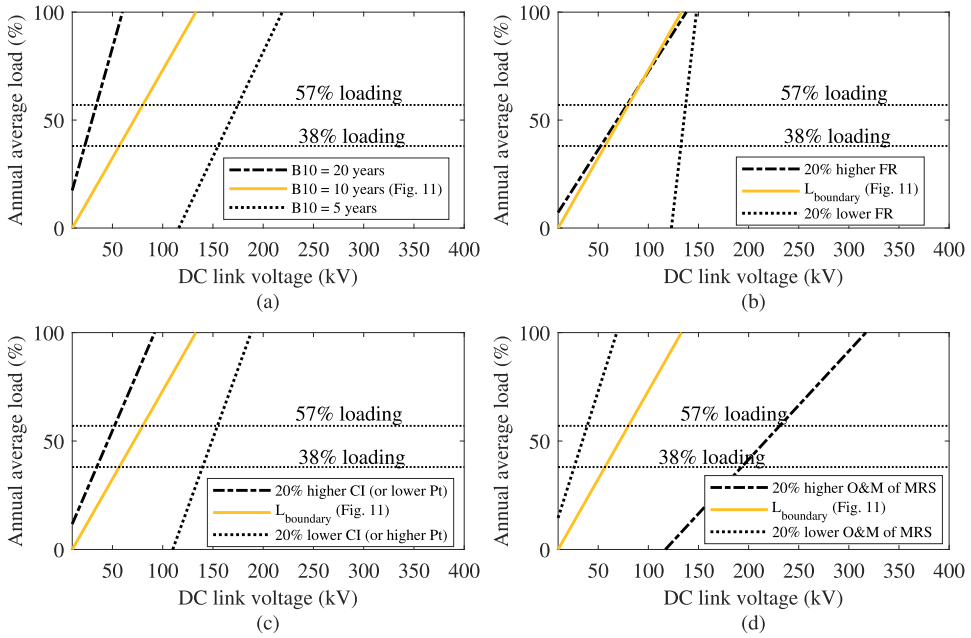

FIGURE. 11. Displacement of L_{boundary} as a function of yearly loading and V_{dc} (ten-year payback) with a variation of (a) B_{10}, (b) FR, (c) CI, and (d) O&M of the MRS.

TABLE 7. OPTIMAL DESIGN OF VARIOUS MMC

Ref	V_{dc}[§] (kV)	Power (MW)	Red (%)	Saving by applying MRS[‡]	
				$P_{l,ave}$ = 38%	$P_{l,ave}$[†] = 57%
[17]	54	30	ARS (31)	109 K€	278.7 K€
[35]	100	100	ARS (32)	606.5 K€	577.7 K€
[36]	300	210	ARS (10)	935.8 K€	948.2 K€
[33]	320	500	ARS (8)	4.624 M€	5.163 M€
[37]	400	800	ARS (8)*	1.793 M€	3.742 M€
[37]	640	1200	ARS (8)*	3.156 M€	5.976 M€
[38]	640	1000	ARS (20)	3.954 M€	4.318 M€

§ pole to pole voltage * 8% redundancy is assumed
† Annual average loading of MMC shown in Fig. 8
‡ The savings are calculated for B_{10} = 10 years and includes operational losses and CI

TABLE 8. ADVANTAGES AND DISADVANTAGES OF MRS COMPARED TO THE EXISTING REDUNDANCY STRATEGIES

Advantages	Disadvantages
• Improved reliability with higher B10 lifetime. • Flexibility in choosing the number of active and spare redundant SMs. • Reduced operational losses and better efficiency. • Applicable across various conditions, allowing for accurate cost estimation and optimal design.	• Complexity in implementation. • High sensitivity to the exact cost of O&M. • SRS can achieve higher efficiency in some scenarios. • Requires detailed and well-planned maintenance schedule.

from 12 to 470.7 MVA. Therefore, appropriate switch ratings should have been selected, as provided in Table 10 (see the Appendix). The results depicted in Fig. 12 illustrate that the boundary line changes trivially ($m = 7.8\ \mu$, $V_{\text{ref}} = 10$ kV),

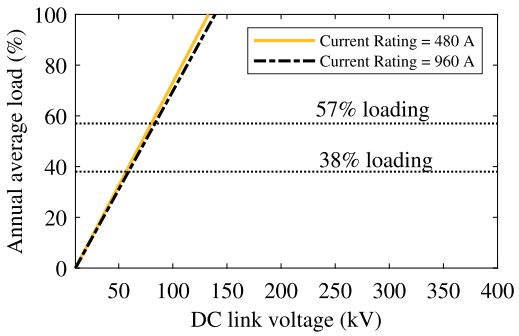

FIGURE. 12. Sensitivity of the obtained results for feasibility boundary for the SRS and the MRS with higher rating switches.

which is negligible. It can be concluded that the selection of MRS over other redundancy strategies is independent of the current rating and primarily hinges on the loading and dc-link voltage. It is worth noting that the same conclusions were drawn in our previous study [23], highlighting that switch rating selection remains independent of the current rating of the MMC.

V. PRACTICALITY AND OPERATIONAL CHALLENGES

MTTF_{arm} considering $T_{\text{O\&M}}$ is given as follows [19]:

$$\text{MTTF}_{\text{arm}} = \frac{\int_0^{T_{\text{O\&M}}} R_{\text{arm-x}}(t)dt}{1 - R_{\text{arm-x}}(T_{\text{O\&M}})}. \tag{14}$$

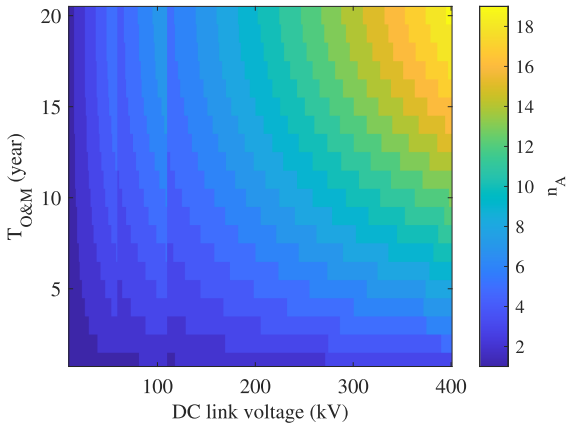

FIGURE. 13. Required number of n_A in each arm for the MRS scheme as a function of dc-link voltage and $T_{O\&M}$ at 100% loading for MTTF = 20 years.

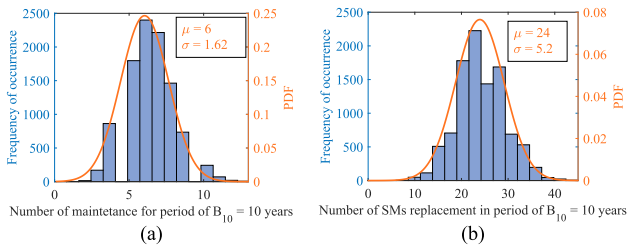

FIGURE. 14. MCS results (10 000 trials) for MMC with $k = 48$ and $n_A = 2$ within the period of $B_{10} = 10$ years. (a) Distribution of the required number of maintenance. (b) Distribution of a number of faulty SMs that is going to be changed.

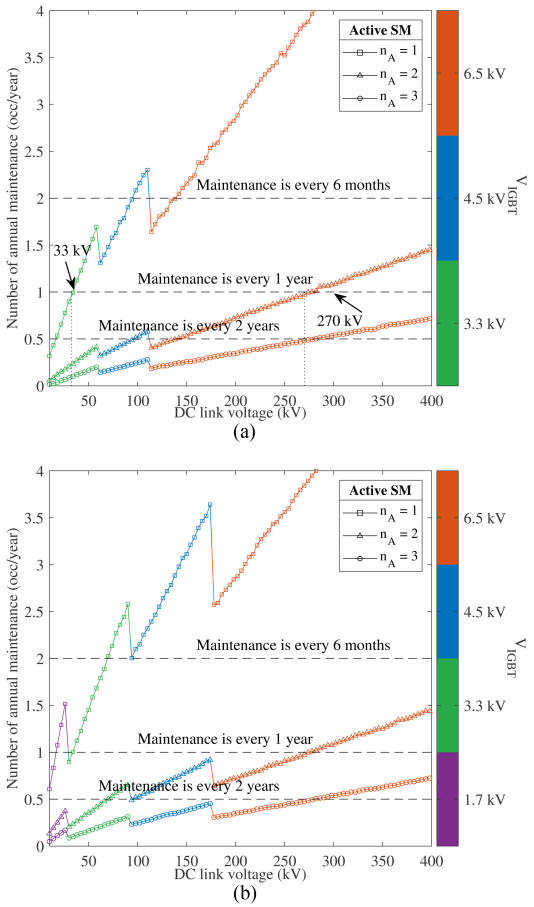

FIGURE. 15. MCS results (10 000 trials) for estimating the number of maintenance frequency in the period of $B_{10} = 10$ years as a function of dc-link voltage at (a) 100% loading and (b) 38% loading.

In Fig. 13, the required number of active redundant SM (n_A) is shown for the MRS scheme considering the required MTTF as a function of V_{dc} and $T_{O\&M}$. It can be observed that n_A must be increased to increase $T_{O\&M}$, which will consequently reduce the O&M costs for the MRS.

This tradeoff is investigated in more detail using the MCS. Fig. 14 shows an example of 10 000 trials for a given MMC with $k = 48$ and $n_A = 2$, demonstrating that maintenance is required approximately six times over a ten-year B_{10} lifetime.

These findings are extrapolated to various MMC configurations. Fig. 15 presents the annual maintenance requirements operating at 100% and 38% annual loading as a function of V_{dc}. Based on the results of Fig. 15(a), it is suggested that if the expected number of maintenance is once per year for a specific application, each arm of the MMC should include one active SM in the V_{dc} range of 10–33 kV. For dc-link voltages ranging from 33 to 270 kV, two active SMs are required per arm to ensure operational continuity. For V_{dc} between 270 and 400 kV, three active redundant SMs ($n_A = 3$) are necessary. The same results can be applied if the annual average loading is 38% [see Fig. 15(b)]. Also, note that the appropriate switch rating is considered according to [23], which depends on annual loading and V_{dc}. This is evident in Fig. 15, where variations occur based on the annual loading of the converter, resulting in dips. Specifically, at 38% loading [see Fig. 15(b)], these dips take place at V_{dc} values of 28, 90, and 177 kV. These variations are attributed to changes in modularity induced by the utilization of different switch ratings. By adhering to these guidelines, the uninterrupted operation of the MMC can be guaranteed, and the maximum number of spare SMs can be shared. However, it is important to note that the expected maintenance intervals in certain applications may differ, such as every two years or every six months, as shown in Fig. 15. The MRS scheme remains applicable in such cases, with the corresponding number of n_A in each arm. Similarly, the MCS methodology can estimate the number of SM failures within a specified period. For instance, as shown in Fig. 16, the expected number of failed SMs can be estimated over a ten-year (B_{10}) period. As observed in Fig. 16, an increase in the number of active redundant SMs (n_A) within each arm results in a reduction in the number of faulty SMs experiencing a lifetime of $B_{10} = 10$ years. This decrease is attributed to the decreased voltage stress across the SMs. However, it is essential to note that the multiplication of n_A by a factor of 6 contributes to an increase in the CI of the MMC. Similar to the observations in Fig. 15, dips around 60 and 120 kV are evident, associated with changes in modularity.

Therefore, implementing the MRS enables the derivation of an optimal design for the MMC across various applications. This optimization, aligned with the O&M planning of

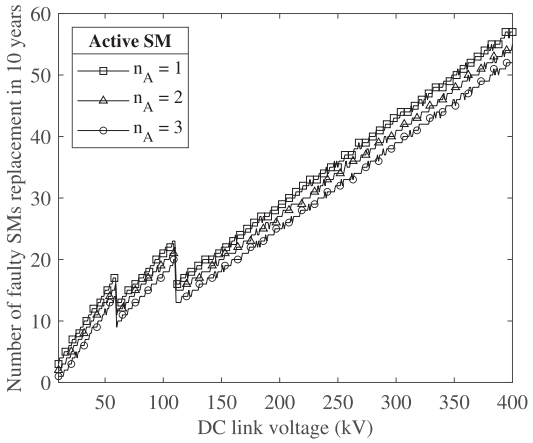

FIGURE. 16. MCS results (10 000 trials) for estimating the number of faulty SM within the period of $B_{10} = 10$ years as a function of dc-link voltage (at 100% loading).

the MMC, results in reduced operational losses and a lower CI. Table 7 showcases the application of the MRS scheme to previously published work and the amount of money that can be saved in $B_{10} = 10$ years. Through considerations of dc-link voltage, annual loading, and O&M planning (assuming maintenance occurs every year), this approach facilitates the accurate estimation of the optimal switch rating, arm-level redundancy (n_A), and spare SMs (n_S) for the replacement of faulty SMs.

In summary, the comprehensive analysis presented in this study is encapsulated in Table 8, which outlines the key advantages and disadvantages of the MRS.

VI. CONCLUSION

The developed analytical model estimates the weighted reliability of the proposed scheme based on two probability distribution functions for converter failure as a function of time. Unlike ARS and SRS, this assessment method is needed because the converter reliability function structurally changes when the redundancy strategy is modified depending on the available spare and active SMs for MRS. Sensitivity analysis indicates that the proposed scheme becomes relatively more economically viable when the required B_{10} lifetime increases. Some dependence on increasing dc-link voltage is also observed, especially for higher B_{10} lifetime. The economic viability is greater when higher component costs are considered. Furthermore, this economic boundary between the MRS and the SRS for a ten-year payback has relatively limited dependence on the variation in component FR. Also, the economic viability of the proposed scheme is independent of the power capacity, which was validated by using different switches with higher current ratings. It was shown that the MRS scheme becomes less favorable if its O&M cost is higher than other redundancy schemes. The effectiveness and applicability of the MRS scheme are validated by proposing the MCS, in which the optimum number of active redundant SMs in each arm is determined following the expected maintenance plan. The MCS also estimates the number of failed SMs by emulating real-life scenarios. The efficacy of the MRS is demonstrated through its application in previously published studies.

APPENDIX

In this section, details regarding the chosen switches are provided in Table 9 for a current rating of 480 A. In addition, Table 10 outlines the switches selected when the current rating of the MMC is increased to 960 A.

TABLE 9. SWITCH CHOICE RATING CURRENT OF 480 A

V_{IGBT} (kV)	Model
1.2	FF450R12ME4
1.7	FF450R12ME4
3.3	FF450R33TE3
4.5	FZ800R45KL3
6.5	FZ500R65KE3

TABLE 10. SWITCH CHOICE RATING CURRENT OF 960 A

V_{IGBT} (kV)	Model
1.2	FF600RME4C
1.7	FF1000R17IE4P
3.3	FZ1000R33HE3BPSA1
4.5	FZ1000R45KL3B5
6.5	FZ500R65KE3 (Two parallel)

REFERENCES

[1] M. Alharbi and S. Bhattacharya, "Scale-up methodology of a modular multilevel converter for HVDC applications," *IEEE Trans. Ind. Appl.*, vol. 55, no. 5, pp. 4974–4983, Sep./Oct. 2019.

[2] M. A. Perez, S. Ceballos, G. Konstantinou, J. Pou, and R. P. Aguilera, "Modular multilevel converters: Recent achievements and challenges," *IEEE Open J. Ind. Electron. Soc.*, vol. 2, pp. 224–239, 2021.

[3] F. B. Ajaei and R. Iravani, "Dynamic interactions of the MMC-HVDC grid and its host AC system due to AC-side disturbances," *IEEE Trans. Power Del.*, vol. 31, no. 3, pp. 1289–1298, Jun. 2016.

[4] J. Xu, C. Zhao, Y. Xiong, C. Li, Y. Ji, and T. An, "Optimal design of MMC levels for electromagnetic transient studies of MMC-HVDC," *IEEE Trans. Power Del.*, vol. 31, no. 4, pp. 1663–1672, Aug. 2016.

[5] H. Wang and F. Blaabjerg, "Reliability of capacitors for DC-link applications in power electronic converters—An overview," *IEEE Trans. Ind. Appl.*, vol. 50, no. 5, pp. 3569–3578, Sep./Oct. 2014.

[6] S. S. Manohar, A. Sahoo, A. Subramaniam, and S. K. Panda, "Condition monitoring of power electronic converters in power plants—A review," in *Proc. IEEE 20th Int. Conf. Elect. Mach. Syst.*, 2017, pp. 1–5.

[7] M. Ahmadi, A. Shekhar, and P. Bauer, "Reconfigurability, modularity and redundancy trade-offs for grid connected power electronic systems," in *Proc. IEEE 20th Int. Power Electron. Motion Control Conf.*, 2022, pp. 35–41.

[8] R. Billinton, S. Aboreshaid, and M. Fotuhi-Firuzabad, "Well-being analysis for HVDC transmission systems," *IEEE Trans. Power Syst.*, vol. 12, no. 2, pp. 913–918, May 1997.

[9] L. Guo, Y. Ding, M. Bao, C. Shao, P. Wang, and L. Goel, "Nodal reliability evaluation for a VSC-MTDC-based hybrid AC/DC power system," *IEEE Trans. Power Syst.*, vol. 35, no. 3, pp. 2300–2312, May 2020.

[10] J. Guo, X. Wang, Z. Bie, and Y. Hou, "Reliability modeling and evaluation of VSC-HVDC transmission systems," in *Proc. IEEE PES Gen. Meeting Conf. Expo.*, 2014, pp. 1–5.

[11] J. Xu, P. Zhao, and C. Zhao, "Reliability analysis and redundancy configuration of MMC with hybrid submodule topologies," *IEEE Trans. Power Electron.*, vol. 31, no. 4, pp. 2720–2729, Apr. 2016.

[12] J. Guo, J. Liang, X. Zhang, P. D. Judge, X. Wang, and T. C. Green, "Reliability analysis of MMCs considering submodule designs with individual or series-operated IGBTs," *IEEE Trans. Power Del.*, vol. 32, no. 2, pp. 666–677, Apr. 2017.

[13] J. Xu, L. Wang, D. Wu, H. Jing, and C. Zhao, "Reliability modeling and redundancy design of hybrid MMC considering decoupled sub-module correlation," *Int. J. Elect. Power Energy Syst.*, vol. 109, pp. 690–698, 2019.
[14] J. Xu, H. Jing, and C. Zhao, "Reliability modeling of MMCs considering correlations of the requisite and redundant submodules," *IEEE Trans. Power Del.*, vol. 33, no. 3, pp. 1213–1222, Jun. 2018.
[15] X. Xie et al., "Reliability modeling and analysis of hybrid MMCs under different redundancy schemes," *IEEE Trans. Power Del.*, vol. 36, no. 3, pp. 1390–1400, Jun. 2021.
[16] J. Guo, X. Wang, J. Liang, H. Pang, and J. Gonçalves, "Reliability modeling and evaluation of MMCs under different redundancy schemes," *IEEE Trans. Power Del.*, vol. 33, no. 5, pp. 2087–2096, Oct. 2018.
[17] G. Abeynayake, G. Li, T. Joseph, J. Liang, and W. Ming, "Reliability and cost-oriented analysis, comparison and selection of multilevel MVdc converters," *IEEE Trans. Power Del.*, vol. 36, no. 6, pp. 3945–3955, Dec. 2021.
[18] H. Li et al., "Cost and reliability optimization of modular multilevel converter with hybrid submodule for offshore DC wind turbine," *Int. J. Elect. Power Energy Syst.*, vol. 120, 2020, Art. no. 105994.
[19] B. Wang, X. Wang, Z. Bie, P. D. Judge, X. Wang, and T. C. Green, "Reliability model of MMC considering periodic preventive maintenance," *IEEE Trans. Power Del.*, vol. 32, no. 3, pp. 1535–1544, Jun. 2017.
[20] P. Tu, S. Yang, and P. Wang, "Reliability- and cost-based redundancy design for modular multilevel converter," *IEEE Trans. Ind. Electron.*, vol. 66, no. 3, pp. 2333–2342, Mar. 2019.
[21] J. E. Huber and J. W. Kolar, "Optimum number of cascaded cells for high-power medium-voltage AC–DC converters," *IEEE Trans. Emerg. Sel. Topics Power Electron.*, vol. 5, no. 1, pp. 213–232, Mar. 2017.
[22] J. V. M. Farias, A. F. Cupertino, V. de Nazareth Ferreira, H. A. Pereira, S. I. Seleme, and R. Teodorescu, "Reliability-oriented design of modular multilevel converters for medium-voltage STATCOM," *IEEE Trans. Ind. Electron.*, vol. 67, no. 8, pp. 6206–6214, Aug. 2020.
[23] M. Ahmadi, A. Shekhar, and P. Bauer, "Switch voltage rating selection considering cost-oriented redundancy and modularity-based trade-offs in modular multilevel converter," *IEEE Trans. Power Del.*, vol. 38, no. 4, pp. 2831–2842, Aug. 2023.
[24] P. Yu, W. Fu, L. Wang, Z. Zhou, G. Wang, and Z. Zhang, "Reliability-centered maintenance for modular multilevel converter in HVDC transmission application," *IEEE Trans. Emerg. Sel. Topics Power Electron.*, vol. 9, no. 3, pp. 3166–3176, Jun. 2021.
[25] F. Feng et al., "Dynamic preventive maintenance strategy for MMC considering multi-term thermal cycles," *Int. J. Elect. Power Energy Syst.*, vol. 116, 2020, Art. no. 105560.
[26] J. Wylie, M. C. Merlin, and T. C. Green, "Analysis of the effects from constant random and wear-out failures of sub-modules within a modular multi-level converter with varying maintenance periods," in *Proc. IEEE 19th Eur. Conf. Power Electron. Appl.*, 2017, pp. P.1–P.10.
[27] A. Shekhar, T. B. Soeiro, Y. Wu, and P. Bauer, "Optimal power flow control in parallel operating AC and DC distribution links," *IEEE Trans. Ind. Electron.*, vol. 68, no. 2, pp. 1695–1706, Feb. 2021.
[28] A. Shekhar, L. B. Larumbe, T. B. Soeiro, Y. Wu, and P. Bauer, "Number of levels, arm inductance and modulation trade-offs for high power medium voltage grid-connected modular multilevel converters," in *Proc. IEEE 10th Int. Conf. Power Electron. ECCE Asia*, 2019, pp. 1–8.
[29] K. Ilves, S. Norrga, L. Harnefors, and H.-P. Nee, "On energy storage requirements in modular multilevel converters," *IEEE Trans. Power Electron.*, vol. 29, no. 1, pp. 77–88, Jan. 2014.
[30] *Reliability Prediction of Electronic Equipment: MIL-HDBK-217D* (ser. Military Standardization Handbook), Department of Defense, Washington, DC, USA, 1983.
[31] R. Billinton and R. N. Allan, *Reliability Evaluation of Engineering Systems: Concepts and Techniques*. New York, NY, USA: Springer, 1992.
[32] J. V. M. Farias, A. F. Cupertino, H. A. Pereira, S. I. Seleme, and R. Teodorescu, "On converter fault tolerance in MMC-HVDC systems: A comprehensive survey," *IEEE Trans. Emerg. Sel. Topics Power Electron.*, vol. 9, no. 6, pp. 7459–7470, Dec. 2021.
[33] A. Shekhar, T. B. Soeiro, L. Ramírez-Elizondo, and P. Bauer, "Offline reconfigurability based substation converter sizing for hybrid AC–DC distribution links," *IEEE Trans. Power Del.*, vol. 35, no. 5,, pp. 2342–2352, Oct. 2020.
[34] J. Kang et al., "On exploiting active redundancy of a modular multilevel converter to balance reliability and operational flexibility," *IEEE Trans. Power Electron.*, vol. 34, no. 3, pp. 2234–2243, Mar. 2019.
[35] H. Kim et al., "Exploiting redundant energy of MMC–HVDC to enhance frequency response of low inertia AC grid," *IEEE Access*, vol. 7, pp. 138485–138494, 2019.
[36] R. Li, L. Yu, L. Xu, and G. P. Adam, "Coordinated control of parallel DR-HVDC and MMC-HVDC systems for offshore wind energy transmission," *IEEE Trans. Emerg. Sel. Topics Power Electron.*, vol. 8, no. 3, pp. 2572–2582, Sep. 2020.
[37] M. Alharbi, S. Isik, and S. Bhattacharya, "A novel submodule level fault-tolerant approach for MMC with integrated scale-up architecture," *IEEE J. Emerg. Sel. Topics Ind. Electron.*, vol. 2, no. 3, pp. 343–352, Jul. 2021.

MIAD AHMADI (Student Member, IEEE) received the B.Sc. degree from Razi University, Kermanshah, Iran, in 2016, and the M.Sc. degree from the Politecnico di Milano, Milan, Italy, in 2019, both in electrical engineering. He is currently working toward the Ph.D. degree in electrical engineering with the DC Systems, Energy Conversion and Storage Group, Delft University of Technology, Delft, The Netherlands.

In 2019, he was an R&D intern with Supergrid Institute, Villeurbanne, France, where he evaluated the reliability of the bus-bar system in high-voltage systems. His research interests include the reliability of power systems, the reliability of power electronics, and the integration of renewable energy sources.

ADITYA SHEKHAR (Member, IEEE) received the bachelor's (Hons.) degree from the National Institute of Technology, Surat, India, in 2010, and the M.Sc. (*cum laude*) and Ph.D. degrees from the Delft University of Technology, Delft, The Netherlands, in 2015 and 2020, respectively, all in electrical engineering.

He is currently an Assistant Professor with the DC systems, Energy Conversion and Storage Group, Department of Electrical Sustainable Energy, Delft University of Technology.

PAVOL BAUER (Senior Member, IEEE) received the master's degree in electrical engineering from the Technical University of Kosice, Kosice, Slovakia, in 1985, and the Ph.D. degree in electrical engineering from the Delft University of Technology, Delft, The Netherlands, in 1995.

From 2002 to 2003, he was with KEMA (DNV GL), Arnhem, The Netherlands, where he worked on different projects related to power electronics applications in power systems. He is currently a Full Professor with the Department of Electrical Sustainable Energy, Delft University of Technology, where he is also the Head of DC Systems, Energy Conversion, and Storage Group. He is also a Professor with the Brno University of Technology, Brno, Czech Republic, and an Honorary Professor with the Politehnica University Timişoara, Timişoara, Romania. He has authored or coauthored more than 120 journal articles and 500 conference papers in his research field. He is an author or coauthor of eight books, holds seven international patents, and organized several tutorials at international conferences. He has worked on many projects for the industry concerning wind and wave energy, power electronic applications for power systems such as Smarttrafo, as well as HVDC systems, and projects for smart cities such as photovoltaic (PV) charging of electric vehicles, PV and storage integration, and contactless charging. He participated in several Leonardo da Vinci and H2020 and Electric Mobility Europe EU projects as a Project Partner (ELINA, INETELE, E-Pragmatic, Micact, Trolley 2.0, OSCD, P2P, and Progressus) and a Coordinator (PEMCWebLab.com-Edipe, SustEner, and Eranet DCMICRO).

Dr. Bauer is the Former Chairman of Benelux IEEE Joint Industry Applications Society, Power Electronics Society, and Power Engineering Society Chapter, the Chairman of the Power Electronics and Motion Control Council, a Member of the Executive Committee of the European Power Electronics Association, and a Member of the International Steering Committee at numerous conferences.